

Multinuclear (^{13}C , ^{31}P , ^{77}Se) Magnetic Resonance and Infrared Spectroscopic Studies of the Interaction of $\text{W}(\text{CO})_4(\text{NO})\text{I}$ with Potentially Bidentate Group 15 and Mixed Group 15/Group 16 Donor Ligands. Electrochemical Studies on Some Group 15 Donor Ligand Derivatives

Alan M. Bond,^{*1} Ray Colton,^{*2} and Penny Panagiotidou²

Division of Chemical and Physical Sciences, Deakin University, Waurn Ponds, Victoria 3217, Australia, and the Department of Inorganic Chemistry, University of Melbourne, Parkville, Victoria 3052, Australia

Received December 28, 1987

A series of potentially bidentate group 15 donor ligands, L-L (L-L = $\text{Ph}_2\text{P}(\text{CH}_2)_x\text{PPh}_2$, $x = 1$, dpm; $x = 2$, dpe; $x = 3$, dpp; $x = 4$, dpb; $\text{Ph}_2\text{AsCH}_2\text{CH}_2\text{PPh}_2$, ape), and mixed group 15/group 16 donor ligands, L-E (E = S, Se; L-E = $\text{Ph}_2\text{PCH}_2\text{P}(\text{E})\text{Ph}_2$, dpmS, dpmSe; L-E = $\text{Ph}_2\text{AsCH}_2\text{CH}_2\text{P}(\text{E})\text{Ph}_2$, apeS, apeSe), have been reacted with $\text{W}(\text{CO})_4(\text{NO})\text{I}$. The products $\text{W}(\text{CO})_2(\text{NO})(\eta^2\text{-L-L})\text{I}$, $\text{W}(\text{CO})_2(\text{NO})(\eta^2\text{-L-E})\text{I}$, $\text{W}(\text{CO})(\text{NO})(\eta^1\text{-L-L})(\eta^2\text{-L-L})\text{I}$, and $\text{W}(\text{CO})(\text{NO})(\eta^1\text{-L-E})(\eta^2\text{-L-E})\text{I}$ were characterized by elemental analysis and infrared and NMR (^{31}P , ^{77}Se) spectroscopies. Electrochemical oxidation of $\text{W}(\text{CO})(\text{NO})(\eta^1\text{-L-L})(\eta^2\text{-L-L})\text{I}$ (L-L = dpm, ape, dpe) on the voltammetric time scale in dichloromethane (0.1 M Bu_4NClO_4) at platinum is dependent on the identity of L-L, being either a two-electron step or two one-electron steps. In all cases, however, a reduction response is observed on the reverse scan whose potential varies markedly with temperature. The oxidation state (I) species is identified as $[\text{W}(\text{CO})(\text{NO})(\eta^1\text{-L-L})(\eta^2\text{-L-L})\text{I}]^+$ and the two-electron oxidation product is $[\text{W}(\text{CO})(\text{NO})(\text{L-L})_2\text{I}]^{2+}$, but its isomeric form is unknown. However, on the longer time scale of controlled potential electrolysis or chemical oxidation the isolated products are *trans*- $[\text{W}(\text{NO})(\eta^2\text{-L-L})_2\text{I}]^{2+}$ in all cases. These species can be electrochemically or chemically reduced to $\text{W}(\text{NO})(\eta^2\text{-L-L})\text{I}$ which in turn can be reoxidized to the dipositive cation. The reduction and oxidation potentials for these reactions differ by over 500 mV so that these systems are chemically reversible but electrochemically irreversible in the Nernstian sense.

Introduction

$\text{W}(\text{CO})_4(\text{NO})\text{I}^3$ reacts with 1 mol equiv of dpm (dpm = $\text{Ph}_2\text{PCH}_2\text{PPh}_2$) to give *cis*- $\text{W}(\text{CO})_2(\text{NO})(\eta^2\text{-dpm})\text{I}^4$. Other workers have reported analogous compounds containing dpe (dpe = $\text{Ph}_2\text{PCH}_2\text{CH}_2\text{PPh}_2$). Robinson and Swanson⁵ prepared *cis*- $\text{M}(\text{CO})_2(\text{NO})(\text{dpe})\text{Cl}$ (M = Mo, W) by the action of nitrosyl chloride on $\text{M}(\text{CO})_3(\text{MeCN})_3$ followed by addition of dpe, while Johnson and co-workers⁶ prepared a series of *cis*- $\text{M}(\text{CO})_2(\text{NO})(\text{dpe})\text{X}$ (X = Cl, Br, I) complexes by the reaction of nitrosyl and halide ions on $\text{M}(\text{CO})_4(\text{dpe})$.

At elevated temperatures *cis*- $\text{W}(\text{CO})_2(\text{NO})(\text{dpm})\text{I}$ reacts with further dpm to give $\text{W}(\text{CO})(\text{NO})(\eta^1\text{-dpm})(\eta^2\text{-dpm})\text{I}^4$ but other compounds of this type with different potentially bidentate ligands have not been reported.

The aim of this work was to produce other examples of complexes of the above types, and similar compounds with unsymmetrical ligands, whose structures could be unambiguously determined by modern spectroscopic techniques. In the first part of this paper the reactions of $\text{W}(\text{CO})_4(\text{NO})\text{I}$ with other bidentate group 15 donor atom ligands (L-L) (L-L = dpe, $\text{Ph}_2\text{CH}_2\text{CH}_2\text{PPh}_2$, $\text{Ph}_2\text{AsCH}_2\text{CH}_2\text{PPh}_2$, ape; $\text{Ph}_2\text{PCH}_2\text{CH}_2\text{CH}_2\text{PPh}_2$, dpp; $\text{Ph}_2\text{PCH}_2\text{CH}_2\text{CH}_2\text{CH}_2\text{PPh}_2$, dpb) are described together with reactions with mixed group 15/group 16 donor atom ligands (L-E, E = S, Se)

(L-E = $\text{Ph}_2\text{PCH}_2\text{P}(\text{E})\text{Ph}_2$, dpmE = dpmS, dpmSe; $\text{Ph}_2\text{AsCH}_2\text{CH}_2\text{P}(\text{E})\text{Ph}_2$, apeE = apeS, apeSe). Extensive infrared and multinuclear (^{13}C , ^{31}P , ^{77}Se) magnetic resonance spectroscopies are used to characterize the products.

Oxidative electrochemical studies of group 6 metal carbonyl complexes have been investigated extensively in the past few years.⁷ Commonly, carbonyl compounds undergo chemically and electrochemically reversible one-electron oxidation processes to produce 17-electron species. The less common two-electron electrochemical oxidation processes of 18-electron carbonyl complexes are generally irreversible and are usually accompanied by ligand addition, leading to an overall retention of the 18-electron configuration for the metal.⁷

The chemical and electrochemical oxidations of $\text{M}(\text{CO})_2(\text{L-L})_2$ (M = Cr, Mo, W; L-L = dpm, dpe) have been investigated,⁸ and the most important species generated are the stable *trans*- $[\text{M}(\text{CO})_2(\text{L-L})_2]^+$ cations. Oxidation of *fac*- and *mer*- $\text{M}(\text{CO})_3(\eta^1\text{-L-L})(\eta^2\text{-L-L})_2$ (M = Mo, W) occurs via two one-electron steps or one two-electron step to produce⁹ seven-coordinate $[\text{M}(\text{CO})_3(\eta^2\text{-L-L})_2]^{2+}$. The electrochemical oxidation of *cis*- $[\text{Mo}(\text{CO})(\text{NO})(\text{dpe})_2]^+$ generates *cis*- $[\text{Mo}(\text{CO})(\text{NO})(\text{dpe})_2]^{2+}$ which rapidly isomerizes to the *trans*²⁺ form,¹⁰ similar to the behavior of the $\text{M}(\text{CO})_2(\text{dpe})_2$ system.

In the second part of this paper the chemical and electrochemical oxidations of some $\text{W}(\text{CO})(\text{NO})(\eta^1\text{-L-L})(\eta^2\text{-L-L})\text{I}$ compounds will be described and compared with the

(1) Deakin University.

(2) University of Melbourne.

(3) Barraclough, C. G.; Bowden, J. A.; Colton, R.; Commons, C. J. *Aust. J. Chem.* **1973**, *26*, 241.

(4) Colton, R.; Commons, C. J. *Aust. J. Chem.* **1973**, *26*, 1498.

(5) Robinson, W. R.; Swanson, M. E. *J. Organomet. Chem.* **1972**, *35*, 315.

(6) Johnson, B. F. G.; Bhaduri, S.; Connelly, N. G. *J. Organomet. Chem.* **1972**, *40*, C36.

(7) Geiger, W. E. *Prog. Inorg. Chem.* **1985**, *33*, 275.

(8) Bond, A. M.; Colton, R.; Jackowski, J. J. *Inorg. Chem.* **1975**, *14*, 274.

(9) Bond, A. M.; Colton, R.; McGregor, K. *Inorg. Chem.* **1986**, *25*, 2378.

(10) Chatt, J.; Kan, C. T.; Leigh, C. J.; Pickett, C. J.; Stanley, D. R. *J. Chem. Soc., Dalton Trans.* **1980**, 2032.

Table I. Analytical Data

	calcd			found		
	C	H	P	C	H	P
<i>cis</i> - $W(CO)_2(NO)(dpmSe)I$	37.7	2.6	7.2	37.9	2.8	7.3
<i>cis</i> - $W(CO)_2(NO)(apeS)I$	38.6	2.8	3.6	38.5	3.1	3.8
$[W(NO)(dpm)_2I](PF_6)_2$	42.9	3.2	13.3	43.9	3.5	13.9
$[W(NO)(ape)_2I](PF_6)_2^a$	41.2	3.2	8.2	41.2	3.8	8.8
$[W(NO)(dpm)_2I](PF_6)_2$	42.9	3.2	13.0	43.9	3.5	13.9

^aAlso: N, 0.9 (1.0); F, 15.0 (14.2); I, 8.4 (8.5).

oxidations of $M(CO)_3(\eta^1-L-L)(\eta^2-L-L)$.

Experimental Section

Materials. Tungsten hexacarbonyl (Pressure Chemical Co.) was dried over P_2O_5 and used without further purification. The L-L ligands (Strem Chemicals Inc.) were used as supplied. All solvents were AR grade and dried over molecular sieves. Tetraabutylammonium perchlorate (TBAP), the supporting electrolyte for electrochemical studies in dichloromethane, was obtained wet with water from South Western Analytical and was dried under vacuum at 70 °C. Tetraethylammonium perchlorate (TEAP) was obtained from G. Frederick Smith.

Preparations. $W(CO)_4(NO)I^3$ and the L-E ligands¹¹ were prepared as described previously. *cis*- $W(CO)_2(NO)(L-L)I$ and *cis*- $W(CO)_2(NO)(L-E)I$ were prepared by refluxing equimolar quantities of $W(CO)_4(NO)I$ and the ligand in chloroform as described previously⁴ for $W(CO)_2(NO)(dpm)_2I$. $W(CO)(NO)(L-L)_2I$ compounds (L-L = dpe, ape) were prepared by interaction of 1:2 proportions of $W(CO)_4(NO)I$ and L-L in *p*-xylene as described previously for $W(CO)(NO)(dpm)_2I$.⁴ The $W(CO)(NO)(L-E)_2I$ compounds were prepared in refluxing benzene. All compounds were recrystallized from dichloromethane/*n*-hexane.

trans- $[W(NO)(L-L)_2I](PF_6)_2$ (L-L = dpm, dpe, ape) were prepared by the action of NOPF₆ on $W(CO)(NO)(L-L)_2I$ in dichloromethane and recrystallized from dichloromethane/*n*-hexane.

Microanalyses were performed by AMDEL Australian Microanalytical Service, and data are given in Table I.

Spectroscopic Measurements. NMR spectra were recorded by using a JEOL FX 100 spectrometer with external ⁷Li lock. Phosphorus-31 NMR spectra were recorded at 40.26 MHz (external reference 85% H_3PO_4) and selenium-77 NMR spectra at 18.99 MHz (external 1 M H_2SeO_3 in H_2O).¹² All NMR spectra were broad-band proton decoupled, and the high frequency positive convention is used for chemical shifts. A JEOL NM 5471 controller was used for temperature control, and the temperatures in the probe were measured with a calibrated platinum resistance thermometer.

Infrared spectra were recorded by using a Jasco A-302 spectrophotometer and calibrated against polystyrene (1601 cm^{-1}).

Electrochemical Measurements. Cyclic voltammograms were recorded in dichloromethane (0.1 M TBAP) or acetone (0.1 M TEAP) by using an EG and G PAR Model 174 polarographic analyzer. A three-electrode system was used with the working and auxiliary electrodes being platinum wire or disks. The reference electrode was Ag/AgCl (CH_2Cl_2 /saturated LiCl) and was separated from the test solution by a salt bridge containing 0.1 M Bu_4NClO_4 in CH_2Cl_2 . Frequent calibration of this reference electrode was carried out against a standard ferrocene solution. Measurements were carried out at 25 °C unless otherwise stated. For variable-temperature cyclic voltammetry, the temperature was regulated by using a dry ice/acetone bath and monitored with a thermocouple. For rotating platinum disk experiments a Metrohm platinum rotating disk assembly with variable rotation rates was used with the same reference and auxiliary electrodes as above.

Controlled potential electrolysis experiments were performed with a PAR Model 173 potentiostat/galvanostat using a platinum gauze working electrode and a platinum auxiliary electrode separated from the bulk solution by a salt bridge containing a Vycor plug. The reference electrode was the same as that used in the voltammetric experiments. All solutions were degassed with

Table II. Infrared Data (cm^{-1}) for Dicarbonyl Compounds

compound	ν_{CO}^a	ν_{NO}^a	$\nu_{P=S}^{b,c}$	$\nu_{P=Se}^{b,c}$
<i>cis</i> - $W(CO)_2(NO)(dpm)I$	2025, 1945	1640		
<i>cis</i> - $W(CO)_2(NO)(dpe)I$	2010, 1940	1630		
<i>cis</i> - $W(CO)_2(NO)(ape)I$	2020, 1945	1635		
<i>cis</i> - $W(CO)_2(NO)(dpp)I$	2025, 1940	1625		
<i>cis</i> - $W(CO)_2(NO)(dpm)I$	2020, 1945	1635		
<i>cis</i> - $W(CO)_2(NO)(dpm)I$	2015, 1950	1630	575 (597)	
<i>cis</i> - $W(CO)_2(NO)(dpm)I$ (dpmSe)I	2020, 1955	1630		510 (529)
<i>cis</i> - $W(CO)_2(NO)(ape)I$	2010, 1940	1625	585 (605)	
<i>cis</i> - $W(CO)_2(NO)(ape)I$	2020, 1940	1640		510 (528)

^aIn dichloromethane. ^bKBr disk. ^cValues for the appropriate free ligand in parentheses.

nitrogen before measurements, except for those conducted under carbon monoxide, and were kept under a nitrogen blanket during the measurements.

Results and Discussion

(a) Preparations and Spectroscopic Studies. (i) Dicarbonyl Compounds. The known compounds *cis*- $W(CO)_2(NO)(L-L)I$ (L-L = dpm, dpe) and the new compounds where L-L = ape, dpp, and dpb were prepared by a method analogous to that given in the literature. Infrared spectra are given in Table II.

Phosphorus-31 and carbon-13 NMR data are given in Table III. Since only singlets are observed in both spectra for each compound, the structure of the complexes can only be that with NO trans to I. Table III also contains the phosphorus coordination chemical shifts, $\Delta[\delta(^{31}P)]$, which decrease steadily with increasing chelate ring size. Thus there is a good correlation between this parameter and ring size, which is different to the previously reported data for $M(CO)_4(L-L)$ systems in which dpm shows anomalous values.¹³

Reaction of $W(CO)_4(NO)I$ and L-E ligands results in the formation of yellow compounds with the constitution $W(CO)_2(NO)(L-E)I$. Infrared data (Table II) show the carbonyl and nitrosyl stretches to be similar to those of the analogous L-L derivatives, implying that the nitrosyl group remains trans to the iodine. Each $W(CO)_2(NO)(L-E)I$ compound displays a single band in the P=S(Se) region whose position is shifted to lower frequency (by 12–20 cm^{-1}) relative to the free ligand, and this is indicative of sulfur or selenium coordination.¹⁴

NMR data for the compounds *cis*- $W(CO)_2(NO)(L-E)I$ are given in Table III. The phosphorus-31 NMR spectrum of *cis*- $W(CO)_2(NO)(dpmSe)I$ consists of two doublets arising from coupling between the two nonequivalent phosphorus atoms. The signals are easily distinguished as the one at higher frequency displays selenium satellites (¹ $J_{P,Se}$ = 605 Hz) while the other has tungsten-183 satellites (¹ $J_{P,W}$ = 260 Hz). The phosphorus-31 coordination chemical shift data for the dpmSe compounds are also given in Table III and have values intermediate between those of the dpm and dpe analogues. For the compounds containing selenium, the selenium-77 NMR spectra are doublets whose chemical shifts are different from those of the free ligands and whose coupling constants are reduced from those of the free ligands, thereby confirming selenium coordination.¹⁴ Two carbon-13 resonances are observed for the carbonyl groups showing that the carbonyl groups are nonequivalent. One resonance is close to the values observed for the corresponding L-L derivatives and the other is at significantly higher frequency. This suggests

(11) Bond, A. M.; Colton, R.; Panagiotidou, P. *Organometallics*, preceding paper in this issue.

(12) Wachli, H. E. *Phys. Rev.* 1953, 90, 331.

(13) Grim, S. O.; Barth, R.; Briggs, W.; Tolman, C. A.; Jesson, J. P. *Inorg. Chem.* 1974, 13, 1095.

(14) Colton, R.; Panagiotidou, P. *Aust. J. Chem.* 1987, 40, 13.

Table III. NMR Data for Dicarbonyl Compounds

compound	$\delta(^{31}\text{P})$	$\Delta[\delta(^{31}\text{P})]$, ^a ppm	$^1J_{\text{W,P}}$, Hz	$\delta(^{13}\text{C})$	$\delta(^{77}\text{Se})$ ^b	$^1J_{\text{P,Se}}$, Hz
<i>cis</i> -W(CO) ₂ (NO)(dpm)I	30.2	52.5	237	208		
<i>cis</i> -W(CO) ₂ (NO)(dpe)I	25.6	39.2	246	206		
<i>cis</i> -W(CO) ₂ (NO)(ape)I	29.7	42.2	249	207		
<i>cis</i> -W(CO) ₂ (NO)(dpp)I	-3.5	14.5	242	205		
<i>cis</i> -W(CO) ₂ (NO)(dph)I	-4.2	12.6	249	206		
<i>cis</i> -W(CO) ₂ (NO)(dpmS)I	16.8 d, 60.7 d	45.6	256	205, 212		
<i>cis</i> -W(CO) ₂ (NO)(dpmSe)I	19.9 d, 40.9 d	47.6	261	204, 211	-1477 d (-1596 d)	601 (732)
<i>cis</i> -W(CO) ₂ (NO)(apeS)I	46.0			207, 214		
<i>cis</i> -W(CO) ₂ (NO)(apeSe)I	33.9			203, 214	-1711 d (-1656 d)	620 (732)

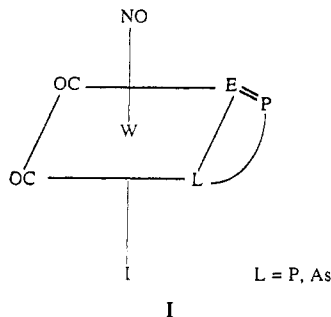
^a $\Delta[\delta(^{31}\text{P})] = \delta(^{31}\text{P})_{\text{compound}} - \delta(^{31}\text{P})_{\text{free ligand}}$. ^b Values for the appropriate free ligand in parentheses.

Table IV. Infrared Data (cm⁻¹) for W(CO)(NO)(η^1 -L-L)(η^2 -L-L)I Compounds

compound	ν_{CO} ^a	ν_{NO} ^a	$\nu_{\text{P}=\text{E}}$ ^{b,c}
W(CO)(NO)(dpm) ₂ I	1915	1600	
W(CO)(NO)(dpe) ₂ I	1918	1600	
W(CO)(NO)(ape) ₂ I	1920	1602	
W(CO)(NO)(dpmS) ₂ I	1915	1618	575, 598 (597)
W(CO)(NO)(dpmSe) ₂ I	1920	1615	515, 530 (529)

^a In dichloromethane. ^b KBr disk. ^c Values for the appropriate free ligand in parentheses.

that the selenium or sulfur atoms are poorer π -acceptors than phosphorus, since the carbonyl group trans to the group 16 donor has a higher chemical shift, implying that it has more electron density.¹⁵ Although no information analogous to the selenium NMR spectra is available for the derivatives containing sulfur-containing ligands, their similar infrared and phosphorus-31 and carbon-13 NMR spectra are sufficient to confirm coordination of sulfur. Thus all the spectroscopic data for *cis*-W(CO)₂(NO)(L-L)I and *cis*-W(CO)₂(NO)(L-E)I compounds are consistent with the stereochemistry shown in structure I.



(ii) **Monocarbonyl Compounds.** W(CO)(NO)(η^1 -dpm)(η^2 -dpm)I was prepared according to the literature method,⁴ and the same method was used to prepare the corresponding complexes with dpe and ape. Infrared spectra are given in Table IV. The nitrosyl stretching frequencies are similar to those of the dicarbonyl species which implies that the nitrosyl is still trans to the iodide.

The phosphorus-31 NMR spectrum of W(CO)(NO)(η^1 -dpm)(η^2 -dpm)I in dichloromethane at room temperature is shown in Figure 1, and data are given in Table V. Four resonances of equal integrated intensities are observed, and this is consistent with the structure shown. Assignment of individual resonances is as follows; the doublet at δ -26, which is close to the resonance for free dpm, is due to P_a and appears as a doublet (J = 49 Hz) due to coupling to P_b. The doublet of doublet of doublets at δ 9.3 (J 's = 24, 49, 132 Hz) is assigned to P_b which is expected to couple to all the other phosphorus atoms. As trans phosphorus-phosphorus coupling constants are

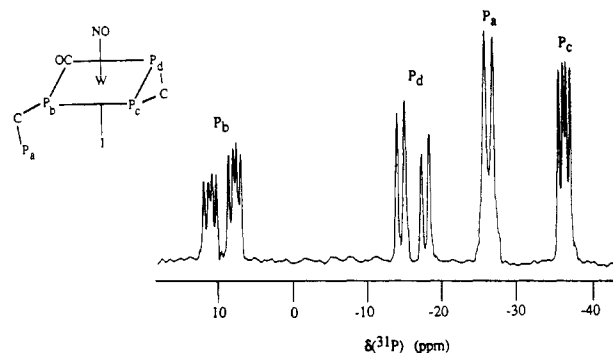


Figure 1. Phosphorus-31 NMR spectrum of W(CO)(NO)(η^1 -dpm)(η^2 -dpm)I in dichloromethane solution at 25 °C.

Table V. Phosphorus-31 NMR Data for W(CO)(NO)(η^1 -L-L)(η^2 -L-L)I Compounds

compound	$\delta(^{31}\text{P})$		$J_{\text{P,P}}$, Hz	
W(CO)(NO)(η^1 -dpm)(η^2 -dpm)I ^a	P _a	-26.0 d	P _{a,b}	49
	P _b	9.3 ddd	P _{b,c}	24
	P _c	-36.5 dd	P _{b,d}	132
	P _d	-16.1 dd	P _{c,d}	39
W(CO)(NO)(η^1 -dpe)(η^2 -dpe)I	P _a	-12.4 d	P _{a,b}	34
	P _b	5.7 ddd	P _{b,c}	17
	P _c	18.4 dd	P _{b,d}	132
	P _d	30.9 dd	P _{c,d}	10
W(CO)(NO)(η^1 -ape)(η^2 -ape)I	P _a	7.8 d	P _{a,b}	132
	P _b	35.6 d		

^a P_a, P_b, etc. as defined in Figure 1. Abbreviations: d, doublet; dd, doublet of doublets; ddd, doublet of doublet of doublets.

known^{16,18} to be greater in magnitude than the corresponding *cis* coupling constants, the largest coupling of 132 Hz is assigned as the coupling constant between P_b and P_d. The remaining coupling constant of 24 Hz is therefore between the *cis* phosphorus atoms P_b and P_c. P_c is expected to appear as a doublet of doublets with two small *cis* coupling constants, and the resonance at δ -36.5 is assigned to this atom. The remaining resonance, a doublet of doublets at δ -16.18 must be due to P_d, and it shows couplings of 132 Hz to P_b and 39 Hz to P_c. Thus the assignment is self consistent and also consistent with the structure shown in Figure 1. The phosphorus-31 NMR spectrum of W(CO)(NO)(dpe)₂I is similar, and data are given in Table V. It is of interest to note that the trans phosphorus-phosphorus coupling constant for this compound is the same as for the dpm derivative, but there are different values for the *cis* coupling constants.

As shown in Table IV, the infrared spectrum of W(CO)(NO)(ape)₂I in the carbonyl and nitrosyl regions is

(16) Pregosin, P. S.; Kunz, R. W. *³¹P and ¹³C NMR of Transition Metal Complexes*; Springer-Verlag: Berlin, 1971.

(17) Bertrand, R. D.; Ogilvie, F. B.; Verkade, J. G. *J. Am. Chem. Soc.* 1970, 92, 1908.

(18) Ogilvie, F. B.; Jenkins, J. M.; Verkade, J. G. *J. Am. Chem. Soc.* 1970, 92, 1916.

(15) Ganscow, O. A.; Vernon, W. D. *Top. ¹³C NMR Spectrosc.* 1976, 2, 270.

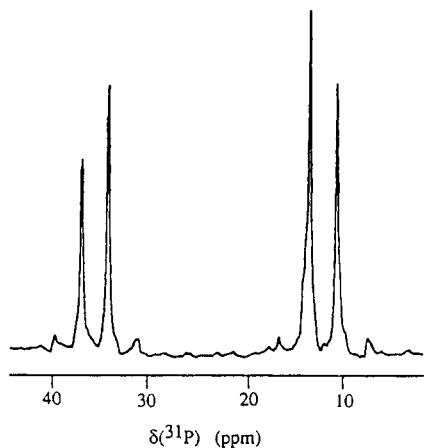
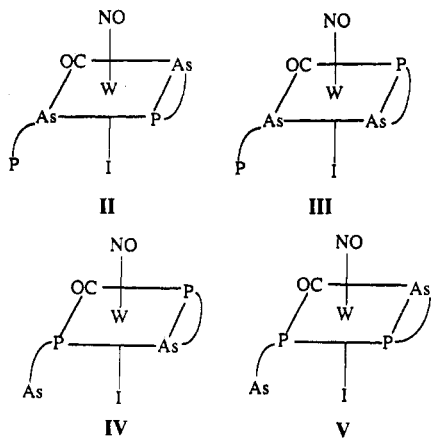


Figure 2. Phosphorus-31 NMR spectrum of $W(CO)(NO)(\eta^1\text{-ape})(\eta^2\text{-ape})I$ in dichloromethane solution at 25 °C.

very similar to that of $W(CO)(NO)(dpm)_2I$, which implies the nitrosyl is trans to the iodide. There are therefore four possible isomers of $cis\text{-}W(CO)(NO)(\eta^1\text{-ape})(\eta^2\text{-ape})I$ as shown in structures II–V. The phosphorus-31 NMR



spectrum of the compound in dichloromethane at room temperature is shown in Figure 2, and it indicates two types of phosphorus atoms that are coupled to each other. For isomers II and III, the spectrum would be expected to be two singlets, with one signal close to the position of the signal for free ape ($\delta -12.5$), suggesting the structure is not II or III. In addition, both doublets display tungsten-183 satellites, indicating that the phosphorus atoms of both ape ligands are coordinated, thereby completely eliminating structures II and III. The coupling constant between the doublets is 132 Hz, exactly the same as the trans coupling constant in the dpm and dpe analogues and to be compared with the cis coupling of 17 Hz in the dpe derivative. Thus the spectrum unequivocally shows the only isomer present is IV. It is interesting that tungsten can discriminate between phosphorus and arsenic coordination in the $\eta^1\text{-ape}$ ligand. The phosphorus-31 NMR spectrum of $W(CO)(NO)nape)_2I$ shows some second-order character with $\Delta\nu_0 = 1118$ Hz, $J_{P,P} = 132$ Hz, and $J/\Delta\nu = 0.12$.

Reaction between $W(CO)_4(NO)I$ and 2 mol equiv of dpmE ligands in refluxing *p*-xylene caused decomposition, but in refluxing benzene yellow compounds of the type $W(CO)(NO)(dpmE)_2I$ were formed. Their infrared spectra (Table IV) in the carbonyl and nitrosyl regions are similar to those of the corresponding L-L ligand derivatives, implying a similar structure. Each compound shows two bands in the P=E region, one at a position very similar to that of the free ligand and the other to lower frequency by 12–14 cm^{-1} showing one dpmE ligand is chelated and

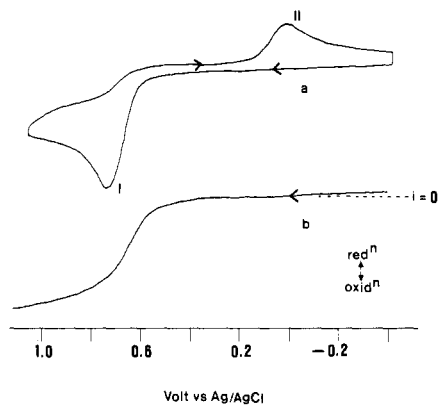
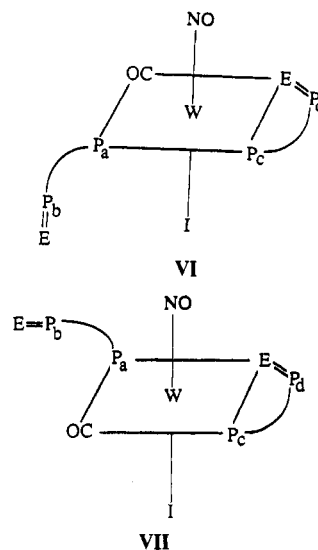


Figure 3. Voltammograms at a platinum electrode for the oxidation of 5×10^{-4} M $W(CO)(NO)(\eta^1\text{-dpm})(\eta^2\text{-dpm})I$ in dichloromethane (0.1 M Bu_4NClO_4) at 25 °C: (a) cyclic voltammogram, scan rate = 200 mV s^{-1} ; (b) rotating disk voltammogram, rotation rate = 2000 rpm.

the other monodentate through phosphorus. There are therefore two possible isomers for $W(CO)(NO)(\eta^1\text{-dpmE})(\eta^2\text{-dpmE})$ as shown in structures VI and VII. In



view of the earlier discussion concerning the carbon-13 NMR spectrum of $W(CO)_2(NO)(dpmE)I$ it would be expected that the carbonyl group trans to phosphorus would be the more readily substituted by additional dpmE, so that isomer VII is the more likely. Unfortunately NMR data is not available because of such extreme insolubility that even for phosphorus-31 an unambiguous spectrum was not obtained after 60 000 accumulations!

(b) **Electrochemical and Chemical Oxidations.** (i) $W(CO)(NO)(\eta^1\text{-dpm})(\eta^2\text{-dpm})I$. Figure 3a shows a cyclic voltammogram for the oxidation of $W(CO)(NO)(dpm)_2I$ in dichloromethane (0.1 M Bu_4NClO_4) at 25 °C at a scan rate of 200 mV s^{-1} . A well-defined irreversible oxidation process (process I) is observed with a peak potential, E_p^{ox} , at 0.74 V vs Ag/AgCl, and no further oxidation processes are observed before the solvent limit. On the reverse scan a reduction peak (process II) is observed with a peak potential, E_p^{red} , at about -0.1 V which is also irreversible as demonstrated by examination of second and subsequent scans. Successive cycles are essentially identical with the first except for the theoretically expected decrease in peak height. Process I and II are chemically irreversible at all scan rates over the range 10–500 mV s^{-1} . The electrochemical data unequivocally show that no iodide (iodine) is liberated after the oxidation step, nor in subsequent

Table VI. Cyclic Voltammetric Data^{a,b} for the Oxidation of 5×10^{-4} M $W(CO)(NO)(\eta^1\text{-dpm})(\eta^2\text{-dpm})I$ at Various Temperatures

process I E_p^{ox} (V) ^c		process II E_p^{red} (V) ^c		T (°C)
CH_2Cl_2	acetone	CH_2Cl_2	acetone	
0.74 (0.24)		-0.10 (-0.60)		25
0.74 (0.24)	0.62 (0.21)	-0.12 (-0.62)	-0.22 (-0.63)	20
0.74 (0.24)	0.64 (0.23)	-0.15 (-0.65)	-0.26 (-0.67)	10
0.74 (0.24)	0.64 (0.23)	-0.18 (-0.68)	-0.27 (-0.68)	0
0.74 (0.24)	0.64 (0.23)	-0.20 (-0.70)	-0.32 (-0.73)	-10
0.75 (0.25)	0.65 (0.24)	-0.30 (-0.80)	-0.38 (-0.79)	-20
0.80 (0.30)	0.68 (0.27)	-0.33 (-0.83)	-0.41 (-0.82)	-30
0.80 (0.30)	0.68 (0.27)	-0.38 (-0.88)	-0.46 (-0.87)	-40
0.80 (0.30)	0.69 (0.28)	-0.42 (-0.92)	-0.52 (-0.93)	-50
0.81 (0.31)	0.69 (0.29)	-0.44 (-0.94)	-0.55 (-0.96)	-60
0.82 (0.32)		-0.47 (-0.97)		-70

^a $E_{1/2}$ for oxidation of ferrocene in $CH_2Cl_2 = 0.50$ V and in acetone = 0.41 V vs Ag/AgCl. ^bScan rate = 200 mV s⁻¹. ^cV vs Ag/AgCl, the values in parentheses are V vs Fc⁺/Fc.

steps, since second and subsequent scans show no evidence for the known^{19,20} redox behavior of this species and independent studies with free dpm showed that it also is not liberated in the oxidation step.

Figure 3b is a platinum rotating disk voltammogram for $W(CO)(NO)(dpm)_2I$, and it shows a single well-defined oxidation process. The limiting current is diffusion-controlled as evidence by the rotation rate dependence (square root dependence). The current per unit concentration is twice that for the known⁹ reversible diffusion-controlled one-electron process for the oxidation of *mer*-Cr(CO)₃(η^1 -dpm)(η^2 -dpm). Since the geometries of Cr(CO)₃(dpm)₂ and $W(CO)(NO)(dpm)_2I$ are similar, it is reasonable to assume that their diffusion coefficients are also similar. On this basis process I is established as a two-electron process.

Process I is irreversible at all temperatures examined (+25 to -70 °C) at a scan rate of 200 mV s⁻¹, and its potential does not vary significantly with temperature. The oxidation peak potentials of ferrocene and other well-defined processes also exhibit relatively small temperature dependence. In contrast, the potential of the reduction step (process II) does vary considerably with temperature. This cannot be due to a temperature-dependent junction potential effect since process I is temperature-independent. Data for both processes at a series of temperatures are given in Table VI. This large and unusual temperature effect will be discussed later.

Electrochemical data in acetone (0.1M Et₄NClO₄) solution are essentially identical with those in dichloromethane when both are related to the potential of the ferrocinium/ferrocene couple as shown in Table VI, thus indicating that the processes are solvent-independent.

Saturating the solution with carbon monoxide has no significant effect on the electrochemical responses in this system on the voltammetric time scale.

Oxidative controlled potential electrolysis of $W(CO)(NO)(dpm)_2I$ in dichloromethane (0.1 M Bu₄NClO₄) at 0.9 V vs Ag/AgCl leads to a color change from yellow to deep yellow, and the electrolysis is complete after the passage of 2.1 ± 0.2 electrons per molecule. However, reductive voltammograms of the oxidized solution do not show process II but instead show a reductive response at -1.0 V vs Ag/AgCl (process III). There is no evidence for the release of iodide or dpm after the oxidation of $W(CO)$ -

Table VII. Infrared and NMR Data in Dichloromethane Solution at 25 °C for $[W(NO)(\eta^2\text{-L-L})_2I]^{2+}$ Cations Prepared by Oxidation of $W(CO)(NO)(\eta^1\text{-L-L})(\eta^2\text{-L-L})I$

compound	ν_{NO} , cm ⁻¹	$\delta(^{31}P)$
$[W(NO)(\eta^2\text{-dpm})_2I]^{2+ a}$	1635	31.6 s
$[W(NO)(\eta^2\text{-dpm})_2I](PF_6)_2^b$	1640	31.2 s, -144.3 sept
$[W(NO)(\eta^2\text{-ape})_2I]^{2+ a}$	1632	37.8 s
$[W(NO)(\eta^2\text{-ape})_2I](PF_6)_2^b$	1640	38.0 s, -144.5 sept
$[W(NO)(\eta^2\text{-dpe})_2I]^{2+ a}$	1630	42.0 s
$[W(NO)(\eta^2\text{-dpe})_2I](PF_6)_2^b$	1630	41.0 s, -144.6 sept

^aPrepared by oxidative controlled potential electrolysis.

^bPrepared by chemical oxidation using NOPF₆.

(NO)(dpm)₂I on the longer coulometric time scale. The fact that the reduction responses for the oxidized solutions are not the same on the voltammetric and coulometric times scales indicates that the product initially formed in the two-electron oxidation on the voltammetric time scale is unstable on the longer coulometric time scale, but the nature of these processes cannot be discussed until after the nature of the oxidation products is established in the next section.

The stable long time scale oxidation product can be studied spectroscopically. Monitoring of the oxidative controlled potential electrolysis experiments by infrared spectroscopy shows that the intensity of the carbonyl stretch of $W(CO)(NO)(dpm)_2I$ gradually decreases and no new carbonyl band appears. In the early stages of the electrolysis the nitrosyl band at 1600 cm⁻¹ appears to broaden slightly, but the final product displays a single band at 1635 cm⁻¹. Thus, the product contains no carbonyl, but nitrosyl is retained. During the course of the electrolysis, the phosphorus-31 NMR spectrum changes from the complex spectrum of $W(CO)(NO)(dpm)_2I$ (Figure 1) to a singlet at δ 31.6. Infrared and NMR data for all the oxidation products for the systems described in this paper are given in Table VII.

It has been shown on many occasions that NOPF₆ is a clean chemical oxidant for zerovalent group 6 metal carbonyl compounds. Oxidation of $W(CO)(NO)(dpm)_2I$ with NOPF₆ gives an intensely yellow solution from which a solid was isolated which analysis showed to have the composition $[W(NO)(dpm)_2I](PF_6)_2$. On redissolving the solid in dichloromethane in the presence of supporting electrolyte, an electrochemical response identical with that of electrochemically oxidized $W(CO)(NO)(dpm)_2I$ is obtained, that is, $[W(NO)(dpm)_2I](PF_6)_2$ gives rise to process III in reductive cyclic voltammograms. In the phosphorus-31 NMR spectrum of the compound the cation gives a singlet at δ 31.2, and integration against the septet due to the anion confirms there are two anions per cation. The small difference in chemical shift between the isolated compound and that prepared in solution by electrochemical techniques may be attributed to ionic strength effects due to the presence of the supporting electrolyte in the latter solutions. The NMR spectrum remains unchanged to -80 °C which strongly suggests that the singlet resonance at room temperature is the true spectrum and not the result of rapid intermolecular exchange. Fluorine-19 NMR spectroscopy shows only the doublet due to the anion and excludes the possibility of fluoride incorporation into the cation.²¹ Similarly proton NMR spectroscopy eliminates the possibility of hydride formation.²² All of the spectroscopic evidence shows that the same product is obtained by long time scale electrochemical oxidation

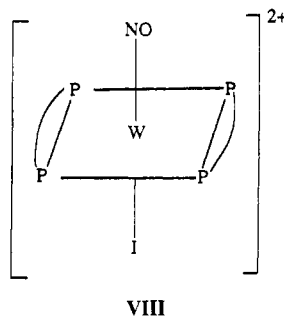
(19) Nakata, R.; Okazaki, S.; Fujinaga, J. *Electroanal. Chem.* 1981, 125, 413.

(20) Popov, A. I.; Geske, D. H. *J. Am. Chem. Soc.* 1958, 80, 1340.

(21) Snow, M. R.; Wimmer, F. C. *Aust. J. Chem.* 1976, 29, 2349.

(22) Connor, J. A.; Riley, P. I.; Rix, C. J. *J. Chem. Soc., Dalton Trans.* 1977, 1317.

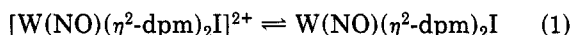
or chemical oxidation using $NOPF_6$ and is consistent only with the structure of the cation being $trans-[W(NO)(\eta^2-dpm)_2I]^{2+}$ (structure VIII). However, this cation is not



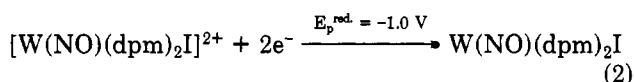
generated on the short voltammetric time scale, so the chemical steps leading to its formation after electron transfer are relatively slow.

As noted above, $[W(NO)(dpm)_2I]^{2+}$ shows a reduction response at -1.0 V in cyclic voltammograms (process III). The solution produced after the two-electron bulk electrolytic reduction of $[W(NO)(dpm)_2I]^{2+}$ at -1.2 V vs Ag/AgCl in dichloromethane (0.1 M Bu_4NClO_4) gives a new voltammetric oxidative response (process IV) at 0.46 V vs Ag/AgCl. Oxidative controlled potential electrolysis of the bulk reduced solution at 0.5 V vs Ag/AgCl regenerates $[W(NO)(dpm)_2I]^{2+}$ quantitatively via a two-electron process. The chemically reversible nature of these processes is demonstrated by the reduction of $[W(NO)(dpm)_2I]^{2+}$ by $LiAlH_4$ in tetrahydrofuran to give the same product as electrochemical reduction, and subsequent oxidation with $NOPF_6$ regenerates $[W(NO)(dpm)_2I]^{2+}$. The obvious formulation to propose for the pale yellow two-electron reduction product of $trans-[W(NO)(dpm)_2I]^{2+}$ is $W(NO)(dpm)_2I$. This compound displays a nitrosyl stretch at 1620 cm^{-1} , and its phosphorus-31 NMR spectrum is a singlet at δ 28.0, showing that it still has the trans configuration.

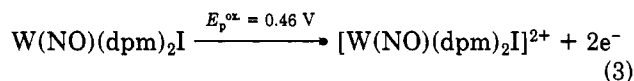
In view of the chemical reversibility of the reaction



the electrochemical reduction process III can be attributed to the reaction



and the oxidation process IV to the reaction



However, as the potentials are so different, processes III and IV represent a couple which is electrochemically irreversible in the Nernstian sense, even though the oxidation and reduction are chemically reversible. This is a rare situation although a similar result has been reported²³ for the two-electron oxidation of ruthenocene to the dication, in which a change of coordination mode for the cyclopentadienyl groups is postulated.

Bubbling carbon monoxide through a solution of the isolated 16-electron compound $[W(NO)(\eta^2-dpm)_2I]^{2+}$ does not form the expected 18-electron carbonyl-containing

Table VIII. Cyclic Voltammetric Data^{a,b} for the Oxidation of 5×10^{-4} M $W(CO)(NO)(\eta^1-ape)(\eta^2-ape)I$ in Dichloromethane and Acetone Solutions at Various Temperatures

process V		process VI	process VII	T (°C)
E_p^{ox} (V) ^c	E_p^{red} (V) ^c	E_p^{ox} (V) ^c	E_p^{red} (V) ^c	
In Dichloromethane (0.1 M Bu_4NClO_4)				
0.84 (0.34)	0.72 (0.22)	1.30 (0.80)	-0.18 (-0.68)	25
0.84 (0.34)	0.72 (0.22)	1.30 (0.80)	-0.24 (-0.74)	10
0.84 (0.34)	0.72 (0.22)	1.30 (0.80)	-0.26 (-0.76)	0
0.85 (0.35)	0.74 (0.24)	1.34 (0.84)	-0.28 (-0.78)	-10
0.85 (0.35)	0.74 (0.24)	1.34 (0.84)	-0.30 (-0.80)	-20
0.86 (0.36)	0.75 (0.25)	1.35 (0.85)	-0.32 (-0.82)	-30
0.86 (0.36)	0.76 (0.26)	1.36 (0.86)	-0.33 (-0.83)	-40
0.87 (0.37)	0.76 (0.26)	1.38 (0.88)	-0.35 (-0.85)	-50
0.87 (0.37)	0.76 (0.26)	1.40 (0.90)	-0.42 (-0.92)	-60
In Acetone (0.1 M Et_4NClO_4)				
0.76 (0.35)	0.65 (0.24)	1.20 (0.79)	-0.26 (-0.67)	25
0.76 (0.35)	0.65 (0.24)	1.21 (0.80)	-0.32 (-0.73)	10
0.77 (0.36)	0.65 (0.24)	1.22 (0.81)	-0.35 (-0.76)	0
0.77 (0.36)	0.66 (0.25)	1.22 (0.81)	-0.36 (-0.77)	-10
0.78 (0.37)	0.66 (0.25)	1.23 (0.82)	-0.38 (-0.79)	-20
0.78 (0.37)	0.67 (0.26)	1.25 (0.84)	-0.39 (-0.80)	-30
0.79 (0.38)	0.67 (0.26)	1.25 (0.84)	-0.44 (-0.85)	-40
0.79 (0.38)	0.68 (0.27)	1.26 (0.85)	-0.45 (-0.86)	-50
0.80 (0.39)	0.68 (0.27)	1.28 (0.87)	-0.51 (-0.92)	-60

^{a-c} As for Table VI.

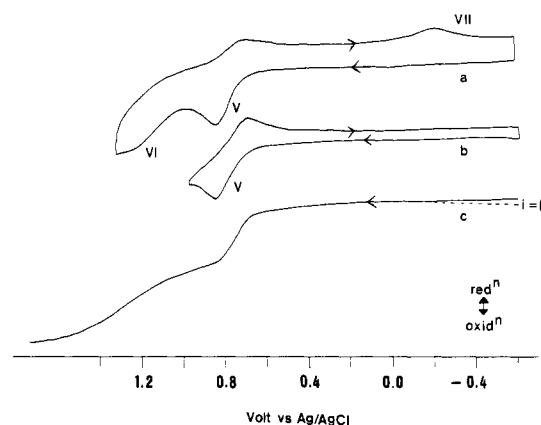


Figure 4. Voltammograms at a platinum electrode for the oxidation of 5×10^{-4} M $W(CO)(NO)(\eta^1-ape)(\eta^2-ape)I$ in dichloromethane (0.1 M Bu_4NClO_4) at 25 °C: (a) cyclic voltammogram (scan rate = 200 $mV s^{-1}$) showing processes V, VI, and VII; (b) cyclic voltammogram (scan rate = 200 $mV s^{-1}$) on switching the potential between processes V and VI; (c) rotating disk voltammogram, rotation rate = 2000 rpm.

compound $[W(CO)(NO)(\eta^2-dpm)_2I]^{2+}$. Also, oxidative-controlled potential electrolysis of $W(CO)(NO)(dpm)_2I$ at 0.9 V vs Ag/AgCl in the presence of 1 atm of carbon monoxide produces neither compounds containing carbon monoxide nor $[W(NO)(\eta^2-dpm)_2I]^{2+}$. The electrolysis is exhaustive after the passage of 4 ± 1 electrons per molecule. The unidentified higher oxidation state compounds retain nitrosyl (infrared evidence) and the phosphine ligands (phosphorus-31 NMR evidence), and no iodine is lost during the course of the electrolysis. Chemical oxidation of $W(CO)(NO)(dpm)_2I$ with $NOPF_6$ in the presence of carbon monoxide produces the same mixture of unidentified non-carbonyl-containing compounds.

(ii) $W(CO)(NO)(\eta^1-ape)(\eta^2-ape)I$. The electrochemical oxidation of $W(CO)(NO)(ape)_2I$ on the voltammetric time scale is distinctly different from that of the analogous dpm compound. Oxidative cyclic voltammograms of $W(CO)(NO)(ape)_2I$ are similar in dichloromethane and acetone, and data are given in Table VIII. Figure 4a shows an oxidative cyclic voltammogram for $W(CO)(NO)(ape)_2I$ in

(23) Diaz, A. F.; Mueller-Westerhoff, U. T.; Nazzari, A.; Tanner, M. J. *Organomet. Chem.* **1982**, *236*, C45.

(24) Clamp, S.; Connelly, N. G.; Taylor, G. E.; Loutit, T. S. *J. Chem. Soc. Dalton Trans.* **1980**, 2162.

(25) Geiger, W. E.; Rieger, P. H.; Tulyathan, B.; Rausch, M. D. *J. Am. Chem. Soc.* **1984**, *106*, 7000 and references cited therein.

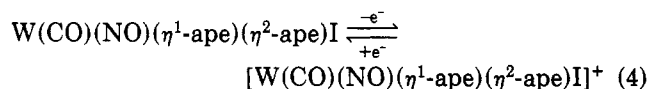
(26) Bond, A. M.; Colton, R. *Inorg. Chem.* **1976**, *15*, 2036.

dichloromethane (0.1 M Bu_4NClO_4) at 25 °C. Two well-defined waves (processes V and VI) of approximately the same height are observed at 0.84 and 1.30 V vs Ag/AgCl, and a reduction response (process VII) is observed on the reverse scan at -0.18 V vs Ag/AgCl. Processes VI and VII are irreversible. When the potential is switched between processes V and VI (Figure 4b), process V is seen to be chemically reversible for all scan rates examined (50–500 mV s^{-1}) and process VII is absent, which shows that process VII must arise from a product of process VI.

As the temperature is lowered to -60 °C, process V remains chemically reversible, processes VI and VII remain irreversible but the potential for process VII varies considerably with temperature, showing a substantial similarity to the behavior of process II in the dpm system, as shown in Table VIII.

Processes V and VI are also observed in the platinum rotating disk experiments (Figure 4c). Process V has the same shape as the known reversible one-electron oxidation of ferrocene; the process is therefore defined as chemically and electrochemically reversible. Process V is extremely well-defined while process VI is drawn out, but after the solvent blank is corrected for, the limiting current per unit concentration is identical for both processes. Comparison of the limiting current per unit concentration with that for the known one-electron oxidation of *mer*- $\text{Cr}(\text{CO})_3(\eta^1\text{-dpm})(\eta^2\text{-dpm})$ and the known two-electron oxidation of *fac*- $\text{Mo}(\text{CO})_3(\eta^1\text{-dpm})(\eta^2\text{-dpm})^9$ provides further evidence that processes V and VI are both one-electron oxidation steps under the conditions of Figure 4.

Process V is therefore consistent with the chemically reversible oxidation process



Further oxidation of the 17-electron cation to oxidation state (II) apparently does not produce a stable isostructural 16-electron cation on the time scale of this experiment but rather a species or mixture of species whose reduction constitutes process VII and which parallels the reduction process for related species in the dpm system.

When dichloromethane solution of $\text{W}(\text{CO})(\text{NO})(\text{ape})_2\text{I}$ is saturated with carbon monoxide, process V increases slightly in height (scan rate 200 mV s^{-1}) and its reversibility is partially lost, but processes VI and VII are drastically modified. Process VI shifts to less positive potential, and its height is decreased. Process VI is similarly decreased in height, and at least three new reduction processes are observed on the reverse scans of cyclic voltammograms. This suggests that a range of products can be formed after electron transfer in the presence of carbon monoxide. Process V is independent of the addition of ape and iodide to the solution, but the effect of these ligands on process VI could not be determined since both ape and iodide are themselves oxidized in the vicinity of process VI.

Oxidative-controlled potential electrolysis of 2×10^{-3} M to 5×10^{-4} M solutions of $\text{W}(\text{CO})(\text{NO})(\text{ape})_2\text{I}$ at 1.0 V vs Ag/AgCl (between processes V and VI) in dichloromethane (0.1 M Bu_4NClO_4) is accompanied by successive color changes from yellow to pink to orange. Exhaustive oxidative electrolysis in this solvent occurs with an n value of 4 ± 1 . The electrolysis proceeds smoothly to the approximately $n = 2$ value with the current gradually decreasing as expected, but it does not fall to zero. Controlled potential electrolysis results are concentration-dependent and are not highly reproducible, and they indicate that a number of follow-up reactions occur after charge transfer on this longer time scale. When the electrolysis is stopped

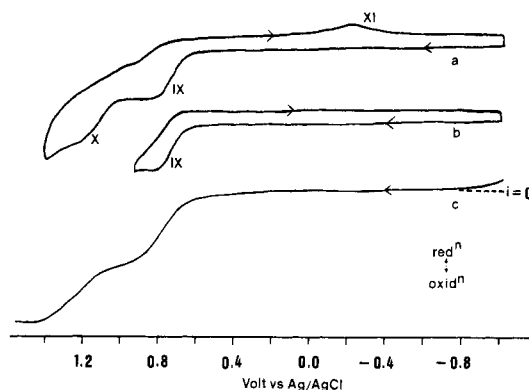


Figure 5. Voltammograms at a platinum electrode for the oxidation of 5×10^{-4} M $\text{W}(\text{CO})(\text{NO})(\eta^1\text{-dpe})(\eta^2\text{-dpe})\text{I}$ in dichloromethane (0.1 M Bu_4NClO_4) at 25 °C: (a) cyclic voltammogram (scan rate = 200 mV s^{-1}) showing processes IX, X, and XI; (b) cyclic voltammogram (scan rate = 200 mV s^{-1}) on switching the potential between processes X and XI; (c) rotating disk voltammogram, rotation rate = 2000 rpm.

after an apparent transfer of two electrons per molecule and the solution examined by cyclic voltammetry, it is observed that some of the starting material remains, that is, process V is still present. The voltammograms are extremely complex and exhibit numerous reduction processes that are time-dependent. The final dominant time-independent reduction process (process VIII) occurs at -0.85 V vs Ag/AgCl. This is a new process not observed on the short time scale of oxidative cyclic voltammetry on $\text{W}(\text{CO})(\text{NO})(\text{ape})_2\text{I}$. The phosphorus-31 NMR spectrum of the solution after electrolysis to the $n = 2$ stage consists of a singlet at δ 37.8 and signals due to remaining $\text{W}(\text{CO})(\text{NO})(\text{ape})_2\text{I}$. This new product is obviously diamagnetic, but the other species detected electrochemically are probably paramagnetic since they do not appear in the NMR spectrum.

Chemical oxidation of $\text{W}(\text{CO})(\text{NO})(\text{ape})_2\text{I}$ by NOPF_6 in dichloromethane produces an orange solution with a similar infrared spectrum ($\nu_{\text{NO}} = 1640 \text{ cm}^{-1}$ and no carbonyl band) as the major long term product of electrochemical oxidation; see Table VII. The compound was isolated as its PF_6^- salt by precipitation with *n*-hexane, and its phosphorus-31 NMR spectrum shows a singlet at δ 38.0, similar to that shown by the electrochemically produced species, and a septet due to PF_6^- . Integration shows there are two anions per cation. This ratio was also confirmed by elemental analysis so the isolated product must be $[\text{W}(\text{NO})(\eta^2\text{-ape})_2\text{I}](\text{PF}_6)_2$. When redissolved in dichloromethane (0.1 M Bu_4NClO_4), the isolated product gave a reduction response identical with process VIII.

As in the case of the dpm system, either electrochemical or chemical oxidation of $\text{W}(\text{CO})(\text{NO})(\text{ape})_2\text{I}$ in the presence of carbon monoxide gives rise to unidentified higher oxidation state products which do not contain carbon monoxide.

(iii) $\text{W}(\text{CO})(\text{NO})(\eta^1\text{-dpe})(\eta^2\text{-dpe})\text{I}$. Figure 5a shows the oxidative cyclic voltammogram of $\text{W}(\text{CO})(\text{NO})(\text{dpe})_2\text{I}$ at 25 °C in dichloromethane (0.1 M Bu_4NClO_4) at a scan rate of 200 mV s^{-1} . Two well-defined oxidation waves are observed at 0.84 and 1.25 V vs Ag/AgCl (processes IX and X), and a reduction wave (process XI) is observed on the reverse scan at -0.2 V. Processes X and XI are irreversible, and on switching the potential between processes IX and X (Figure 5b), process IX is observed to display only a barely visible degree of reversibility and process XI is absent. Thus process XI must arise from the products of process X. As the temperature is lowered, process IX

Table IX. Voltammetric Data^{a,b} for the Oxidation of 5 × 10⁻⁴ M W(CO)(NO)(η¹-dpe)(η²-dpe)I in Dichloromethane and Acetone Solutions at Various Temperatures

process IX		process X	process XI	T (°C)
E _p ^{ox.} (V) ^c	E _p ^{red.} (V) ^c	E _p ^{ox.} (V) ^c	E _p ^{red.} (V) ^c	
In Dichloromethane (0.1 M Bu ₄ NClO ₄)				
0.84 (0.34)		1.16 (0.66)	-0.20 (-0.70)	25
0.84 (0.34)		1.18 (0.68)	-0.22 (-0.72)	10
0.84 (0.34)		1.20 (0.70)	-0.23 (-0.73)	0
0.84 (0.34)		1.22 (0.72)	-0.24 (-0.74)	-10
0.84 (0.34)		1.26 (0.76)	-0.26 (-0.76)	-20
0.84 (0.34)	0.72 (0.22)	1.30 (0.80)	-0.28 (-0.78)	-30
0.86 (0.36)	0.72 (0.22)	1.34 (0.84)	-0.34 (-0.84)	-40
0.86 (0.36)	0.72 (0.22)	1.38 (0.88)	-0.44 (-0.94)	-50
0.86 (0.36)	0.72 (0.22)	1.40 (0.90)	-0.50 (-1.00)	-60
In Acetone (0.1 M Et ₄ ClO ₄)				
0.76 (0.35)		1.06 (0.65)	-0.28 (-0.69)	25
0.76 (0.35)		1.09 (0.68)	-0.31 (-0.72)	10
0.76 (0.35)		1.11 (0.70)	-0.33 (-0.74)	0
0.76 (0.35)		1.14 (0.73)	-0.35 (-0.76)	-10
0.76 (0.35)		1.16 (0.75)	-0.37 (-0.78)	-20
0.77 (0.36)	0.67 (0.26)	1.23 (0.82)	-0.38 (-0.79)	-30
0.78 (0.37)	0.67 (0.26)	1.26 (0.85)	-0.42 (-0.83)	-40
0.78 (0.37)	0.68 (0.27)	1.28 (0.87)	-0.51 (-0.92)	-50
0.78 (0.37)	0.68 (0.27)	1.32 (0.91)	-0.58 (-0.99)	-60

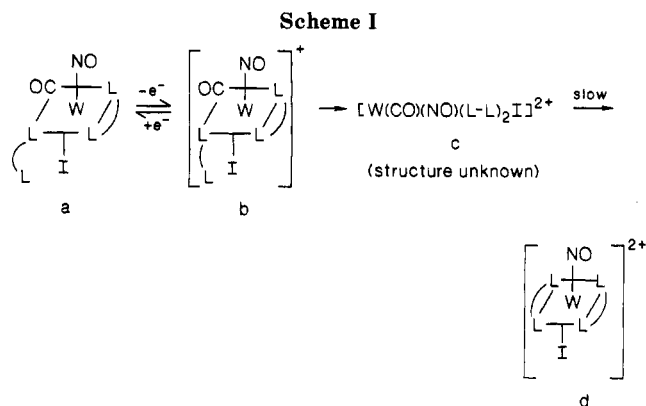
^{a-c} As for Table VI.

begins to show some reversibility, provided the potential is switched before process X, and at -40 °C, it is fully reversible at a scan rate of 200 mV s⁻¹. On scanning the full potential range at low temperatures, processes X and XI remain irreversible and the potential for process XI varies substantially with temperature in a manner similar to processes III and VII. At temperatures below -40 °C the voltammetric behavior of W(CO)(NO)(dpe)₂I closely parallels that of W(CO)(NO)(ape)₂I at room temperature. Electrochemical data are given in Table IX.

Figure 5c shows the results of rotating platinum disk experiments for W(CO)(NO)(ape)₂I at 25 °C. Processes IX and X are both well-defined, and the limiting currents per unit concentration are similar after background correction. Comparison of the current per unit concentration with known one- and two-electron oxidation processes as described earlier confirms that both processes IX and X involve one electron. The contrast between the irreversible one-electron process IX and the irreversible two-electron process I is noteworthy.

The results of oxidative controlled potential electrolysis of W(CO)(NO)(ape)₂I are very similar to those in the ape system. Electrolysis at 1.0 V vs Ag/AgCl (between processes IX and X) in dichloromethane (0.1 M Bu₄NClO₄) is accompanied by successive color changes from yellow to pink to orange. Many reduction waves are observed in the reductive cycle voltammograms of the oxidized solution, and they are time dependent. Monitoring of the solution by infrared spectroscopy shows that carbon monoxide is lost and nitrosyl retained during the oxidative (ν_{NO} = 1630 cm⁻¹). The final major species in the oxidized solution gives a reduction wave at -0.9 V vs Ag/AgCl (process XII) which is not seen on the shorter voltammetric time scale, and its phosphorus-31 NMR spectrum contains a singlet at δ 42, although other minor signals are also observed.

Chemical oxidation of W(CO)(NO)(dpe)₂I by NOPF₆ in dichloromethane produces an orange solution with a nitrosyl band at 1630 cm⁻¹, but no carbonyl band. The compound was isolated as its PF₆⁻ salt which was shown by elemental analysis to be [W(NO)(dpe)₂I](PF₆)₂. Its phosphorus-31 NMR spectrum shows a singlet at δ 41 ppm and the septet due to PF₆⁻, with the integration confirming



the formulation. When redissolved in dichloromethane (0.1 M Bu₄NClO₄), the isolated product gave a reduction response corresponding to process XII. Thus all the data are consistent with the long-term product of electrochemical oxidation and chemical oxidation of W(CO)(NO)(η¹-dpe)(η²-dpe)I is *trans*-[W(NO)(dpe)₂I]²⁺, whose structure is analogous to that of *trans*-[W(NO)(dpm)₂I]²⁺, show in structure VIII.

As with the previous systems, electrochemical or chemical oxidation of W(CO)(NO)(dpe)₂I in the presence of carbon monoxide gave only unidentified higher oxidation state products with loss of the carbonyl group.

General Discussion

The electrochemical oxidations of W(CO)(NO)(η¹-L)(η²-L-L)I compounds on the short voltammetric time scale show a marked dependence upon the identity of L-L. W(CO)(NO)(dpm)₂I gives rise to a single irreversible two-electron oxidation process, while W(CO)(NO)(ape)₂I gives two one-electron oxidation processes, the first of which is reversible. Finally, W(CO)(NO)(dpe)₂I gives two irreversible one-electron oxidation processes at 25 °C with the first becoming reversible below -40 °C. After the transfer of two electrons, all the systems give rise to similar, highly temperature-dependent reduction responses on the reverse scans.

Despite these considerable differences on the voltammetric time scale, all the compounds give similar products on the longer time scales of coulometric and chemical oxidations. The identified major long term products are *trans*-[W(NO)(η²-L-L)₂I]²⁺, and there appears to be degree of commonality in the oxidation mechanisms on the longer time scale. Connelly and co-workers²⁴ have isolated the compounds Cr(NO)(η²-dpe)₂F and Mo(NO)(η²-dpe)₂Cl that could be oxidized by one-electron processes to the stable Cr(I) and Mo(I) complexes [Cr(NO)(η²-dpe)₂F]BF₄ and [Mo(NO)(η²-dpe)₂Cl]PF₆, but no analogous tungsten complexes were reported. In this work with tungsten as the metal and iodide as the halide no evidence for stable tungsten(I) compounds of the type [W(NO)(L-L)₂I]⁺ was obtained.

A generalized partial mechanism for both electrochemically and chemically generated [W(NO)(L-L)₂I]²⁺ is shown in Scheme I. It is convenient to discuss the ape system first since in this case there is direct evidence from the voltammetric studies for the formation of [W(CO)(NO)(η¹-ape)(η²-ape)I]⁺, compound b, which can be oxidized at fairly positive potential to compound c. After the second electron transfer has occurred, the temperature-dependent reduction response (process VII) occurs.

The large temperature dependence of process VII (and processes II and XI) is very unusual. On the basis of oxidation of analogous compounds, such as M(CO)₃(η¹-L-

L)(η^2 -L-L),⁹ it can be confidently assumed that compound **c** has the empirical formula $[\text{W}(\text{CO})(\text{NO})(\text{ape})_2\text{I}]^{2+}$. However, the isomeric form of this species, and indeed whether it is a six-coordinate 16-electron or seven-coordinate 18-electron species, or whether the nitrosyl group is linear or bent, cannot be determined. The behavior of process VII could have its origin in a temperature-dependent distribution of bent and linear nitrosyl ligand complexes leading to a highly temperature-dependent electron-transfer rate.²⁵ Alternatively, a temperature-dependent distribution of isomers containing (η^1 -ape)(η^2 -ape) and (η^2 -ape)₂ could explain the behavior. In any event, $[\text{W}(\text{CO})(\text{NO})(\text{ape})_2\text{I}]^{2+}$ slowly decomposes via an unknown mechanism to form the isolated 16-electron product $[\text{W}(\text{NO})(\eta^2\text{-ape})_2\text{I}]^{2+}$ (compound **d**).

The dpm system differs only in the fact that the 17-electron intermediate $[\text{W}(\text{CO})(\text{NO})(\text{dpm})_2\text{I}]^+$ (compound **b** Scheme I) is not directly observed in the voltammetric experiments, and a direct two-electron oxidation of $\text{W}(\text{CO})(\text{NO})(\text{dpm})_2\text{I}$ gives compound **c** directly. Nevertheless, the oxidation probably proceeds through compound **b** which then rapidly disproportionates, a process frequently observed for 17-electron carbonyl systems.^{9,27,28}

The mechanism for oxidation of $\text{W}(\text{CO})(\text{NO})(\eta^1\text{-dpe})(\eta^2\text{-dpe})\text{I}$ at low temperatures is similar to that of $\text{W}(\text{CO})(\text{NO})(\text{ape})_2\text{I}$ at room temperature. However, an

alternative pathway is available to the dpe complex to generate compound **c**, since at room temperature the first oxidation process is irreversible but the reduction response due to compound **c** is still observed. It is palusible that at room temperature the 17-electron W(I) species $[\text{W}(\text{CO})(\text{NO})(\eta^1\text{-dpe})(\eta^2\text{-dpe})\text{I}]^+$, containing the W(I)-NO⁺ linkage, undergoes internal electronic rearrangement to give a six-coordinate W(II)-NO⁰ 16-electron species containing a bent NO ligand. Chelation of the second dpe ligand gives a seven-coordinate W(II) species and a further one-electron oxidation of NO to NO⁺ would give compound **d**. Alternatively, the pendant phosphorus in the six-coordinate 1+ cation could chelate to give a 19-electron seven-coordinate species before the second electron transfer to give compound **d**. Nineteen-electron species have been observed previously in nitrosyl systems.^{25,29}

Oxidation of $\text{M}(\text{CO})_3(\eta^1\text{-L-L})(\eta^2\text{-L-L})$ (M = Mo, W; L-L = dpm, dpe) gives species believed⁹ to be $[\text{M}(\text{CO})_3(\eta^2\text{-L-L})_2]^{2+}$, as fairly stable seven-coordinate 18-electron species. In contrast, two-electron oxidation of $\text{W}(\text{CO})(\text{NO})(\eta^1\text{-L-L})(\eta^2\text{-L-L})\text{I}$ gives the 16-electron $[\text{W}(\text{CO})(\text{L-L})_2\text{I}]^{2+}$ cation as the final stable product. Thus replacing carbonyl by nitrosyl and halide has marked effects on the nature of the thermodynamically stable product.

Acknowledgment. P.P. thanks the Australian Government for a Post Graduate Research Award.

(27) Bagchi, R. N.; Bond, A. M.; Colton, R.; Luscombe, D. L.; Moir, J. E. *J. Am. Chem. Soc.* 1986, 108, 3352.

(28) Pickett, C. J.; Pletcher, D. *J. Chem. Soc., Dalton Trans.* 1975, 879.

(29) Mason, J.; Mingos, D. M. P.; Schaefer, J.; Sherman, D.; Stejskal, E. O. *J. Chem. Soc. Chem. Commun.* 1985, 444.

Characterization of the Organometallic Lewis Acid $(\eta^5\text{-C}_5\text{H}_5)(\text{CO})\text{Fe}(\text{OR}_2)(\eta^2\text{-CH}_2=\text{CHCH}_3)^+\text{BF}_4^-$

Alan R. Cutler* and Alicia B. Todaro

Department of Chemistry, Rensselaer Polytechnic Institute, Troy, New York 12180-3590

Received December 11, 1987

Protonation of the η^3 -allyl complex $\text{Cp}(\text{CO})\text{Fe}(\text{CH}_2\text{CHCH}_2)$ (**10**) with $\text{HBF}_4\cdot\text{OEt}_2$ or $\text{HBF}_4\cdot\text{OMe}_2$ in CH_2Cl_2 (-80°C) affords an extremely reactive organometallic Lewis acid precursor, which degrades above -65°C . The structure assigned to this Lewis acid, on the basis of its ¹¹B and ¹⁹F NMR spectral measurements and of its chemical reactivity, is $\text{Cp}(\text{CO})\text{Fe}(\text{OR}_2)(\text{CH}_2=\text{CHCH}_3)^+\text{BF}_4^-$ (**8**). Similar NMR measurements are also reported for appropriate model compounds containing coordinated fluoroborate [e.g., $\text{Cp}(\text{CO})_2\text{FeF}_2\text{BF}_3$ and $\text{Cp}(\text{CO})_3\text{MoF}_2\text{BF}_3$] or ionic BF_4^- [e.g., $\text{Cp}(\text{CO})_2\text{Fe}(\text{THF})^+\text{BF}_4^-$]. Some potential ligands (e.g., THF) deprotonate **8** back to starting **10**, whereas others (e.g., acetonitrile) readily convert **8** into examples of disubstituted complexes, $\text{Cp}(\text{CO})\text{Fe}(\text{L}_1)(\text{L}_2)^+\text{BF}_4^-$. Excess $\text{P}(\text{OPh})_3$, for example, converts **8** first to the η^2 -propene derivative $\text{Cp}(\text{CO})\text{Fe}(\text{CH}_2=\text{CHCH}_3)\text{P}(\text{OPh})_3^+\text{BF}_4^-$ (**13**) and then in refluxing CH_2Cl_2 to $\text{Cp}(\text{CO})\text{Fe}[\text{P}(\text{OPh})_3]_2^+\text{BF}_4^-$ (**14**). Reactions between **8** and the acetyl complexes $\text{Cp}(\text{CO})(\text{L})\text{FeCOCH}_3$ (L = CO, PPh₃) give the bimetallic μ -(η^1 -C,O)-acetyl compounds $\text{Cp}(\text{CO})(\text{L})\text{Fe}-\text{C}(\text{CH}_3)\text{O}-\text{Fe}(\text{CO})_2\text{Cp}^+\text{BF}_4^-$ (**15**) in low yields, with no evidence of forming μ -(η^2 -C,O)-acetyl derivatives $\text{Cp}(\text{CO})\text{Fe}(\text{CH}_3\text{CO})\text{Fe}(\text{L})\text{Cp}^+\text{BF}_4^-$. The organometallic etherate complex $\text{Cp}(\text{CO})_2\text{Fe}(\text{OMe}_2)^+\text{BF}_4^-$ (**2a**) results through protonolysis of $\text{Cp}(\text{CO})_2\text{FeCH}_3$ with $\text{HBF}_4\cdot\text{OMe}_2$ between -30 and -78°C . This unstable salt decomposes even at -55°C in CH_2Cl_2 or CDCl_3 solution, as monitored by ¹H and ¹⁹F NMR spectroscopy. The ether on **2a** likewise is extremely labile; conditions are reported for replacing it by acetonitrile to give $\text{Cp}(\text{CO})_2\text{Fe}(\text{NCCH}_3)^+\text{BF}_4^-$ (**2c**).

Introduction

The organometallic Lewis acid $\text{Cp}(\text{CO})_2\text{Fe}^+$ or Fp^+ (**1**), which usually is associated with BF_4^- or PF_6^- counterions,

serves as a useful intermediate for generating a wide variety of complexes Fp-L^+ (**2**) (L is a neutral, two-electron donor ligand).¹ This extremely reactive intermediate **1**,